Research Article

Occurrence of Anticyclonic Tornadoes in a Topographically Complex Region of Mexico

Noel Carbajal [ID],[1] **José F. León-Cruz** [ID],[1] **Luis F. Pineda-Martínez** [ID],[2]
José Tuxpan-Vargas [ID],[1] **and Juan H. Gaviño-Rodríguez** [ID][3]

[1]*División de Geociencias Aplicadas, Instituto Potosino de Investigación Científica y Tecnológica A.C., San Luis Potosí, SLP 78216, Mexico*
[2]*Unidad Académica de Ciencias Sociales, Universidad Autónoma de Zacatecas, Zacatecas, ZAC 98066, Mexico*
[3]*Centro Universitario de Investigaciones Oceanológicas, Universidad de Colima, Manzanillo, COL 28860, Mexico*

Correspondence should be addressed to Noel Carbajal; noelc@ipicyt.edu.mx

Tornadoes are violent and destructive natural phenomena that occur on a local scale in most regions around the world. Severe storms occasionally lead to the formation of mesocyclones, whose direction or sense of rotation is often determined by the Coriolis force, among other factors. In the Northern Hemisphere, more than 99% of all tornadoes rotate anticlockwise. The present research shows that, in topographically complex regions, tornadoes have a different probability of rotating clockwise or anticlockwise. Our ongoing research programme on tornadoes in Mexico has shown that the number of tornadoes is significantly higher than previously thought. About 40% of all tornadoes occur in the complex topographic region of the Trans-Mexican Volcanic Belt. Data collected (from Internet videos) on the rotation of tornadoes formed in this region showed that about 50% of them rotated in a clockwise direction, contradicting tornado statistics for most of North America. Time series of the helicity parameter showed that tornadoes formed in topographically complex areas exhibited different behaviours compared to those formed in plains that are related with supercell systems.

1. Introduction

Rotational phenomena in the atmosphere occur at a wide range of scales, from turbulent motions at several centimetres, dust swirls at several metres, tornadoes at hundreds of metres, hurricanes at hundreds of kilometres, and, finally, circulations associated with planetary perturbations at thousands of kilometres. Circulation and vorticity parameters essentially represent two ways of quantifying such rotational processes. Circulation is the line integral of the velocity vector around a closed curve, whereas vorticity is the rotational of the velocity vector. In other words, circulation is a measure of the size of a rotational event, whereas vorticity defines the spinning rate [1]. The vertical component of the relative vorticity, ς, is calculated from horizontal gradients of the velocity vector. The absolute vorticity is calculated as $\omega^{(a)} = \varsigma + f$, where $f = 2\Omega \sin \varphi$ is the

Coriolis parameter, $\Omega = 7.29 \times 10^{-5} \cdot \text{s}^{-1}$ is the angular velocity of Earth, and φ is the latitude. Therefore, vorticity can be related to circulation simply by dividing circulation by the covered area. In this sense, vorticity can also be interpreted as twice the angular velocity of the rotating system. Simple solutions of the equation of motion in natural coordinates reveal that tornadoes of typical scales may have a cyclonic or anticyclonic rotational direction. This solution is called cyclostrophic balance.

Tornadoes are an extremely powerful natural phenomenon defined as "a rotating column of air, in contact with the surface, pendant from a cumuliform cloud, and often visible as a funnel cloud and/or circulating debris/dust at the ground" [2]. Given their unpredictable frequency and scale, as well as their high potential to cause damage, tornadoes are categorised as extreme weather events [3]. Severe storms and tornadoes are closely related. Abundant lower-tropospheric

moisture, steep mid-tropospheric lapse rates, and strong tropospheric wind shear are important elements that influence the formation of tornadoes [4]. Also, high vorticity values, i.e., rotating air masses produced by the interaction of cold and warm fronts, are one of the key factors leading to the development of supercell storms and tornadoes [5].

Generally, the spatial distribution of severe storms and tornadoes coincides with large convergence zones of air masses [6]. These processes often occur on plains, such as on the plains of North America where supercell storms are common. Furthermore, tornadogenesis mainly occurs in supercell systems that are affected by the Coriolis force, which causes tornadoes in the Northern Hemisphere to generally rotate in an anticlockwise direction. However, a large number of tornadoes also occur in non-mesocyclonic systems. It is important to mention that the possibility of anticyclonic events cannot be ruled out. In this respect, Snider [7] carried out the first description of an anticyclonic tornado, and Fujita [1] studied the characteristics of such events. Recently, the features of anticyclonic tornadoes were explained applying radar data [8]. Anticyclonic tornadoes are generally found on the hook echo of anticyclonic supercells in updrafts that take place within a preexisting anticyclonic vortex [9]. Several publications have additionally described the physical and dynamic aspects of tornadoes [10–13]. Recent data on the incidence of tornadoes in the United States (U.S.) indicate that up to 1200 tornadoes may occur per year [14, 15]. But, countries such as Canada [16], India [17], Greece [18], China [19], Spain [20], Brazil [21], and South Africa [22] also have well-documented tornado events. Although statistics on anticyclonic tornadoes around the world are not available, studies have shown that these phenomena are rather rare. Fujita [1] found that, in 27 years, only 29 clockwise-rotating tornadoes were detected in the U.S. Snider [7] similarly found that, of 100 investigated tornadoes, only 1 had an anticyclonic rotation. In recent research works, no information on frequency of anticyclonic tornadoes was found. If one considers the abovementioned average number of tornadoes per year, a very small percentage were anticyclonic. This simple analysis demonstrates the overwhelming dominance of cyclonic tornadoes in the Northern Hemisphere.

2. Study Region

The Trans-Mexican Volcanic Belt (TMVB) is a Neogene volcanic arc built on the southern edge of the North American plate [23]. It extends approximately 900 km from the Pacific Ocean in the west to the Gulf of Mexico in the east, crossing 13 states in Mexico; its width varies from 200 to 300 km. The region is characterised by a complex topography, with mountains reaching heights of more than 5000 m (Figure 1). Also, the TMVB is considered as one of the 14 biogeographic provinces in Mexico and is defined as a transition zone [24]. The region selected for this analysis is located within the zone of influence of the TMVB from 18.80°N, 105.40°W to 21.52°N, 95.79°W.

3. Methodology

An official tornado database does not exist for Mexico, but some efforts have documented tornadoes [25]. We have directed an ongoing data collection programme on tornado events since 2013 based on official reports from the National Weather Service of Mexico, eyewitness reports, social media networks, and newspapers. Every tornado report is validated and entered into our database. This information can be later used as a starting point for research on tornadoes. In the present study, video evidence of the occurrence of tornadoes and their sense of rotation during the 2010–2017 period was obtained from the Internet (YouTube, Twitter, and Facebook). We only considered tornado records that had complete information on the time of occurrence and the coordinates of the event and that were associated with videos evidencing the sense of rotation. To determine the prevailing meteorological conditions during these tornado events, we applied the Weather Research and Forecasting (WRF) model. For this analysis, 11 tornadoes, including 7 anticyclonic and 4 cyclonic tornadoes, were selected. In addition, the tornado of Ciudad Acuña in 2015 is highlighted as reference of a mesocyclonic tornado in a flat region of Mexico.

The WRF model is a numerical weather prediction and atmospheric simulation system designed for research and operational applications [26]. Although the used resolution is not appropriated to resolve tornadoes themselves, the WRF model is an important tool that can show how local systems (mountain-valley circulations or forced convection by topography) and mesoscale systems (cold fronts or moisture fluxes) interact with a tornado formation. Accordingly, the WRF Model has been used in several studies on tornadoes [17, 27–30]. In the present study, the selected reanalysis dataset was the NCEP FNL Operational Model Global Tropospheric Analyses. These data are expressed on a $1 \times 1°$ grid every six hours [31]. All calculations were carried out using similar domain characteristics and physical parameterisations. A mother domain (D1) was created with 100×100 grid points, a 9 km resolution and outputs every 30 minutes. Then, a first nested domain (D2) was generated with 88×88 grid points, a 3 km resolution, and outputs every 30 minutes; finally, a second nested domain (D3) was generated with 76×76 grid points, a 1 km resolution, and outputs every 10 minutes. All simulations were carried out so that the points where tornadoes occurred were centred in space and time. The physical options were selected as follows: WRF single-moment 3-class schemes for microphysics; Dudhia shortwave scheme, RRTM longwave scheme, and MM5 similarity scheme for surface layer options; unified Noah land surface model for land surface options; Yonsei University scheme (YSU) for planetary boundary layer options; and Kain–Fritsch scheme for cumulus parameterisation [32–38].

4. Results

The study of tornadoes in Mexico, a country with complex topography, is relatively incipient. In the 2000–2017 period,
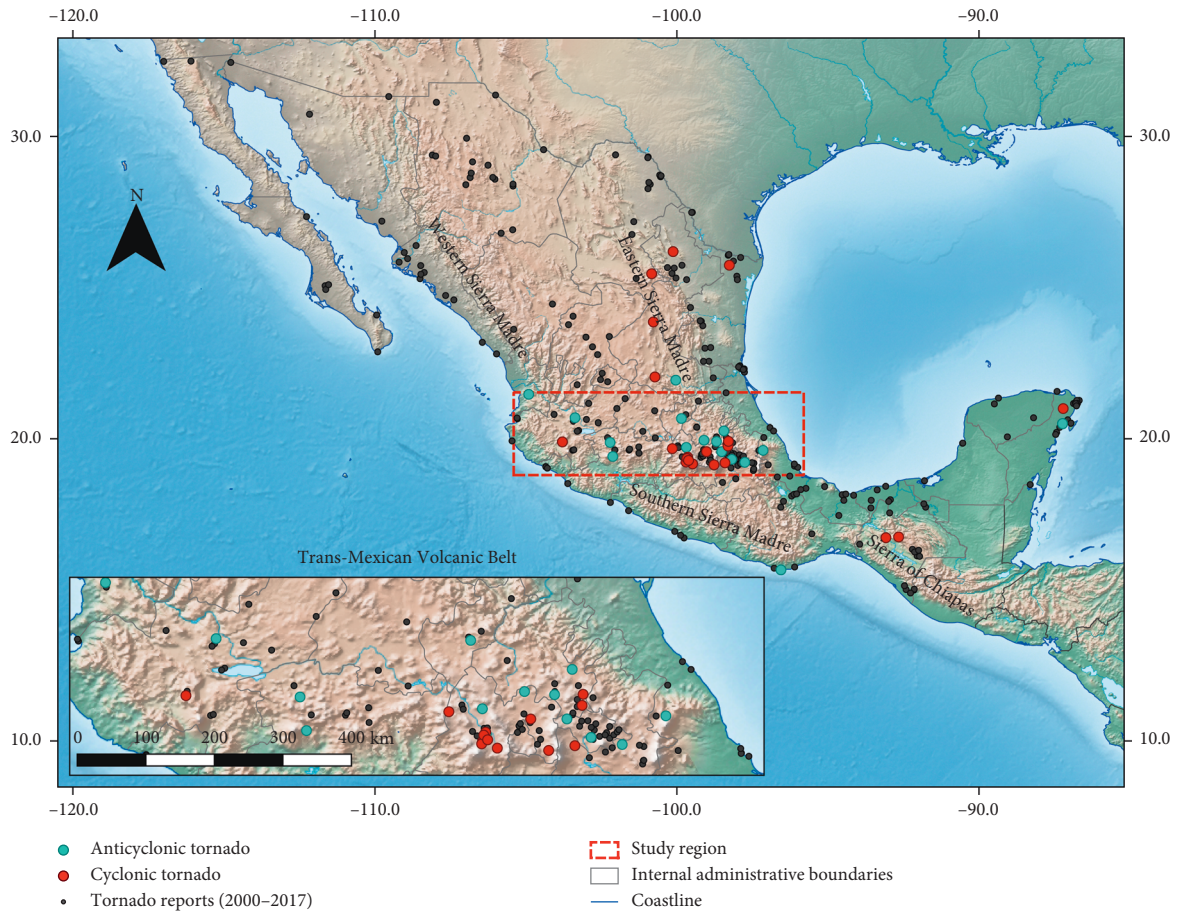
FIGURE 1: Orography of Mexico and spatial distribution of tornadoes originating from 2000 to 2017. The box indicates the region of the Trans-Mexican Volcanic Belt. Cyclonic and anticyclonic tornadoes are marked with red and blue circles, respectively. The names of several important mountain ranges are also indicated. Tornado reports were collected from a previous climatology [25] and our data.

331 tornado events were reported, corresponding with a yearly mean of about 18. In our ongoing data collection programme on the occurrence of tornadoes, up to 30, 50, 46, and 58 tornado events were identified in 2014, 2015, 2016, and 2017, respectively, so the yearly number of tornadoes may be substantially higher. As shown in Figure 1, tornadoes appear across nearly the entire country of Mexico, yet the spatial distribution reveals a clear correspondence with complex orographic features. In particular, a relatively high number of tornadoes occurred within the TMVB region of central Mexico. Also, numerous tornadoes were recorded along the Eastern Sierra Madre. Interestingly, in the flat coastal regions of the Gulf of Mexico and the Yucatan Peninsula, an important number of tornadoes were also recorded. The coastal side of the Western Sierra Madre also frequently experiences tornadoes. However, a simple analysis reveals that about 40% of all documented tornadoes for the 2000–2017 period occurred in the complex orographic region of the TMVB.

Additionally, a careful analysis of 27 audio-visual items with information on tornadoes in the TMVB region for the 2010–2017 period revealed an outstanding fact: 14 tornadoes rotated clockwise (marked with blue circles in Figure 1), whereas 13 rotated anticlockwise (marked with red circles in Figure 1). It seems that tornadoes have the same probability of rotating in either a clockwise or anticlockwise direction in the TMVB. These data records are random in character, as there is no reason to believe that a similar proportion of clockwise- or anticlockwise-rotating tornadoes was purposefully recorded. The criteria for the selection were solely based on the clarity of the sense of rotation and the ability to identify the place of occurrence (in the TMVB) of the visual material uploaded by Mexican individuals. This information allows us to infer that the number of tornadoes that rotate in a clockwise direction is high and that practically all of these tornadoes occur in the TMVB. Table 1 shows the list of documented tornadoes in the TMVB and their corresponding identification, date, place of occurrence, geographic position, and sense of rotation. Video links for each tornado (YouTube, Twitter, and Facebook) are included in the supplementary information. It is important to mention that the tornado marked as I.D. 8 (Table 1) initially exhibited anticyclonic rotation but then shifted to cyclonic rotation. In this case, it likely occurred in the vicinity of a convective zone where both cyclonic and anticyclonic vortexes may have been present.

Several fundamental questions arise as follows: why do so many tornadoes occur along the Trans-Mexican Volcanic

TABLE 1: Summary of tornado events in the Trans-Mexican Volcanic Belt (2010–2017) with video evidence on the sense of rotation (A: anticyclonic; C: cyclonic).

I.D.	Date	Place	Latitude	Longitude	Rotation
1	06/09/2010	Guadalajara, Jalisco (7)	20.690	−103.373	A
2	15/05/2011	Zempoala, Hidalgo (3)	19.914	−98.687	A
3	30/05/2011	Jocotitlán, State of Mexico (4)	19.719	−99.687	A
4	16/03/2012	Toluca de Lerdo, State of Mexico	19.363	−99.631	A
5	22/03/2014	Tangancícuaro, Michoacán (5)	19.882	−102.211	A
6	14/04/2015	Acatlán, Hidalgo (1)	20.264	−98.443	A
7	01/06/2015	San José Chiapa, Puebla (6)	19.224	−97.751	A
8	10/09/2015	Nuevo Parangaricutiro, Michoacán	19.417	−102.122	A
9	27/05/2016	Chiautempan, Tlaxcala (2)	19.323	−98.182	A
10	26/03/2017	Calpulalpan, Tlaxcala	19.578	−98.516	A
11	06/06/2017	Las Vigas de Ramírez, Veracruz	19.621	−97.146	A
12	29/06/2017	Tequixquiac, State of Mexico	19.957	−99.103	A
13	18/07/2017	Xalisco, Nayarit	21.465	−104.905	A
14	06/08/2017	Cadereyta de Montes, Querétaro	20.665	−99.849	A
15	01/06/2012	Ecatepec, State of Mexico (10)	19.577	−99.017	C
16	16/08/2012	Toluca de Lerdo, State of Mexico	19.267	−99.686	C
17	21/05/2014	Santiago Tianguistenco, State of Mexico	19.174	−99.480	C
18	17/08/2014	Almoloya, Hidalgo	19.766	−98.306	C
19	23/03/2016	San José del Rincón, State of Mexico	19.678	−100.151	C
20	21/04/2016	Cuautepec de Hinojosa, Hidalgo (8)	19.919	−98.292	C
21	24/05/2016	Toluca de Lerdo, State of Mexico	19.233	−99.697	C
22	03/08/2016	Tapalpa, Jalisco (11)	19.901	−103.791	C
23	01/05/2017	Amecameca de Juárez, State of Mexico	19.142	−98.769	C
24	17/05/2017	Toluca de Lerdo, State of Mexico (9)	19.395	−99.641	C
25	17/05//2017	Toluca de Lerdo, State of Mexico	19.354	−99.668	C
26	30/05/2017	Huejotzingo, Puebla	19.208	−98.406	C
27	07/08/2017	Toluca de Lerdo, State of Mexico	19.289	−99.614	C

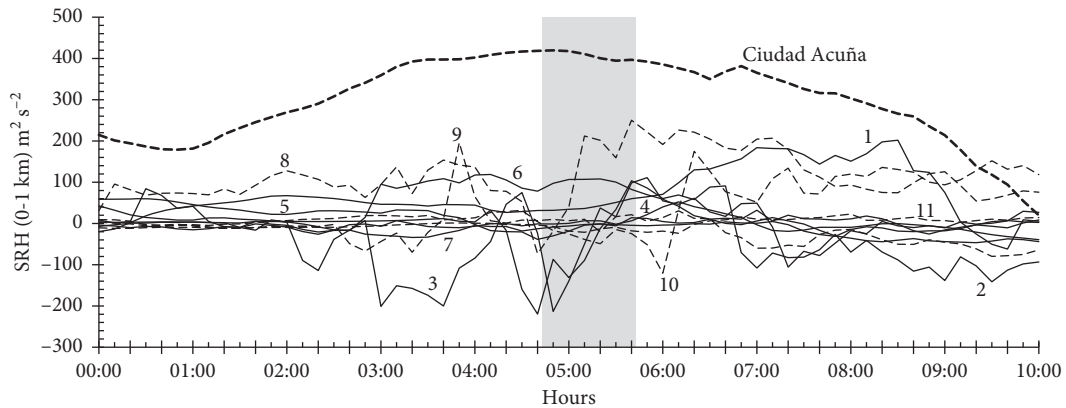Note: the numbers in parentheses indicate the time series shown in Figure 2.

FIGURE 2: Time series of storm-relative helicity (SRH) of 12 tornadoes in the Trans-Mexican Volcanic Belt (TMVB) region: seven clockwise-rotating tornadoes (continuous lines marked as 1 to 7) and 5 anticlockwise-rotating tornadoes (dashed lines marked as 8 to 11) are shown. The Ciudad Acuña event (mesocyclonic tornado) is marked at the top of the graph. The shaded region illustrates the time-period when tornadoes occurred.

Belt? Why do tornadoes have the same probability of rotating clockwise or anticlockwise? And, why do clockwise-rotating tornadoes mostly appear in the TMVB region? We discuss some of the possible answers. The mountain chain of the TMVB represents a significant barrier to frontally propagating meteorological perturbations. In North America, no similar obstacles of this magnitude exist for the propagation of cold or warm air masses. This feature induces

numerous processes of forced convection that may lead to the formation of severe storms. Also, the TMVB separates regions with distinct meteorological characteristics. On the northern side, a highland zone with significant drought is present; this region frequently receives cold air masses. In contrast, the southern side is often influenced by the entrance of moist air masses from the Gulf of Mexico or from the Pacific Ocean. So, the interaction of these air masses with

the intricacies of the complex orography of the TMVB tends to generate favourable conditions for the formation of severe storms and, occasionally, cyclonic or anticyclonic tornadoes, which apparently have a similar probability of occurrence.

Figure 3 displays several relative humidity patterns developed during cyclonic and anticyclonic tornado events in the TMVB. In the first case shown in Figure 3(a) (I.D. 6 in Table 1), an anticyclonic tornado occurred at the boundary between two air masses: a humid air mass from the Gulf of Mexico and a dry air mass occupying the TMVB. Normally, the interaction of these two kinds of air masses initiates an instability process. In Figure 3(b), a humid air mass flowing from the Pacific Ocean towards the TMVB is shown interacting with a drier air mass. Again, an anticyclonic tornado (I.D. 9) occurred near the border separating these two air masses. In Figure 3(c), a cyclonic tornado (I.D. 15) that developed under low relative humidity conditions is shown, but the contrast in relative humidity is of the same order as the tornadoes depicted in Figures 3(a) and 3(b) (I.D. 6 and 9, respectively). Another situation is illustrated in Figure 3(d), showing the prevalence of high relative humidity values during a cyclonic tornado event (I.D. 20). Hence, the hypothesis that interacting air masses influenced by the TMVB, i.e., its orographic intricacies, leads to the formation of tornadoes seems to be correct. Humid air masses flowing from the Pacific Ocean or from the Gulf of Mexico and drier masses from the north often encounter one another in this transition zone. Their interaction appears to significantly contribute towards processes of atmospheric instability and the formation of severe storms and tornadoes. These dynamics may represent one answer to the question of why so many tornadoes occur along the Trans-Mexican Volcanic Belt.

Convection of humid air masses can be induced by convergence processes, or forced convection can be induced by the presence of mountains. In Figure 4, the positions of tornadoes with cyclonic (red points) and anticyclonic (blue points) rotations are shown in the TMVB for the 2010–2017 period. A general inspection reveals that anticyclonic tornadoes overwhelming tend to occur in a particular mountainous area near random geological formations, whereas cyclonic tornadoes are more dominant across extensive valley areas. This qualitative evaluation further confirms that the complex orography of the TMVB plays an important role in determining the sense of rotation of tornadoes formed in this region. Overall, tornadoes seem to have a similar probability of rotating in either a clockwise or anticlockwise direction, as confirmed by the collected videos on tornadoes (Table 1). Although the importance of local dynamical conditions such as valley-mountain circulation, convergence and divergence processes, and convection seems to prevail in the process of tornado formation, mesoscale meteorological circulations also play a role in driving air masses towards the TMVB. Another factor to consider is that the Coriolis force at the latitudes of the TMVB is about half that of Tornado Alley in the U.S. Also, in the TMVB region, tornadoes generally form in areas with mountains as lateral boundaries in contrast to the open plains of the U.S.

Ultimately, tornadoes are hazardous events that can have destructive consequences and pose dangers to the safety and health of individuals inhabiting the regions where they occur. The present study is based on official public records and videos of tornadoes observed by inhabitants, so the results may be related to population density. In Figure 5, the population density in the TMVB region and the position of recorded tornadoes are shown, revealing a close correlation between the positions of recorded tornadoes (black points) and areas with a high population density (reddish areas). This pattern has essentially two implications: first, the tornadoes in this region represent a potential danger for the inhabitants, and second, the number of tornadoes in this region may be markedly higher if one considers that tornadoes may occur in areas with low population density yet remain unreported. Then, the relevant meteorological conditions prevailing during the occurrence of tornadoes and other meteorological dynamics are discussed.

5. Discussion

Relevant meteorological characteristics prevailing during the occurrence and evolution of tornadoes in the TMVB were simulated using the Weather Research and Forecasting (WRF-ARW) model. The results are shown on the nested domain at a resolution of 1 km based on the average 10-minute outputs. The orography of the region suggests that the behaviour of meteorological variables can be complex. In fact, important rotational variables such as vorticity and helicity exhibit a complex behaviour in their temporal and spatial distributions, in contrast to a smooth behaviour of these parameters found in a mesocyclonic system.

Helicity is the vertical integration of the scalar product of the velocity and vorticity vectors; that is, vorticity is included in helicity. The consideration of the velocity vector relative to storm or cloud motion is called storm relative helicity (SRH). SRH is interpreted as the transfer of vorticity from the environment to zones with convective motion [40]. When the values of SRH and convective available potential energy (CAPE) are high, these two elements can regulate the intensification of mesocyclones and the likelihood of tornadogenesis [41]. The integration of SRH within a range of 0-1 km is a good forecast parameter for distinguishing between tornadic supercells and ordinary storms [42]. In Figure 2, time series of SRH are shown for 12 tornadoes, including 7 clockwise-rotating tornadoes (continuous lines) and 5 anticlockwise-rotating tornadoes (dashed lines). Although the tornadoes occurred on different dates under diverse conditions in the TMVB region, a 10-hour period is shown for all of them. The shaded strip indicates the incidence time of tornadoes. A complex behaviour is observed, with SRH values oscillating between approximately -200 and $200 \, \text{m}^2 \cdot \text{s}^{-2}$. Among the cyclonic tornadoes (marked from 8 to 11), positive values are temporally dominant; among the anticyclonic tornadoes (marked from 1 to 7), negative values are dominant. However, the most important characteristic is that the SRH values of both types of tornadoes oscillate around zero. The considered spatial and temporal
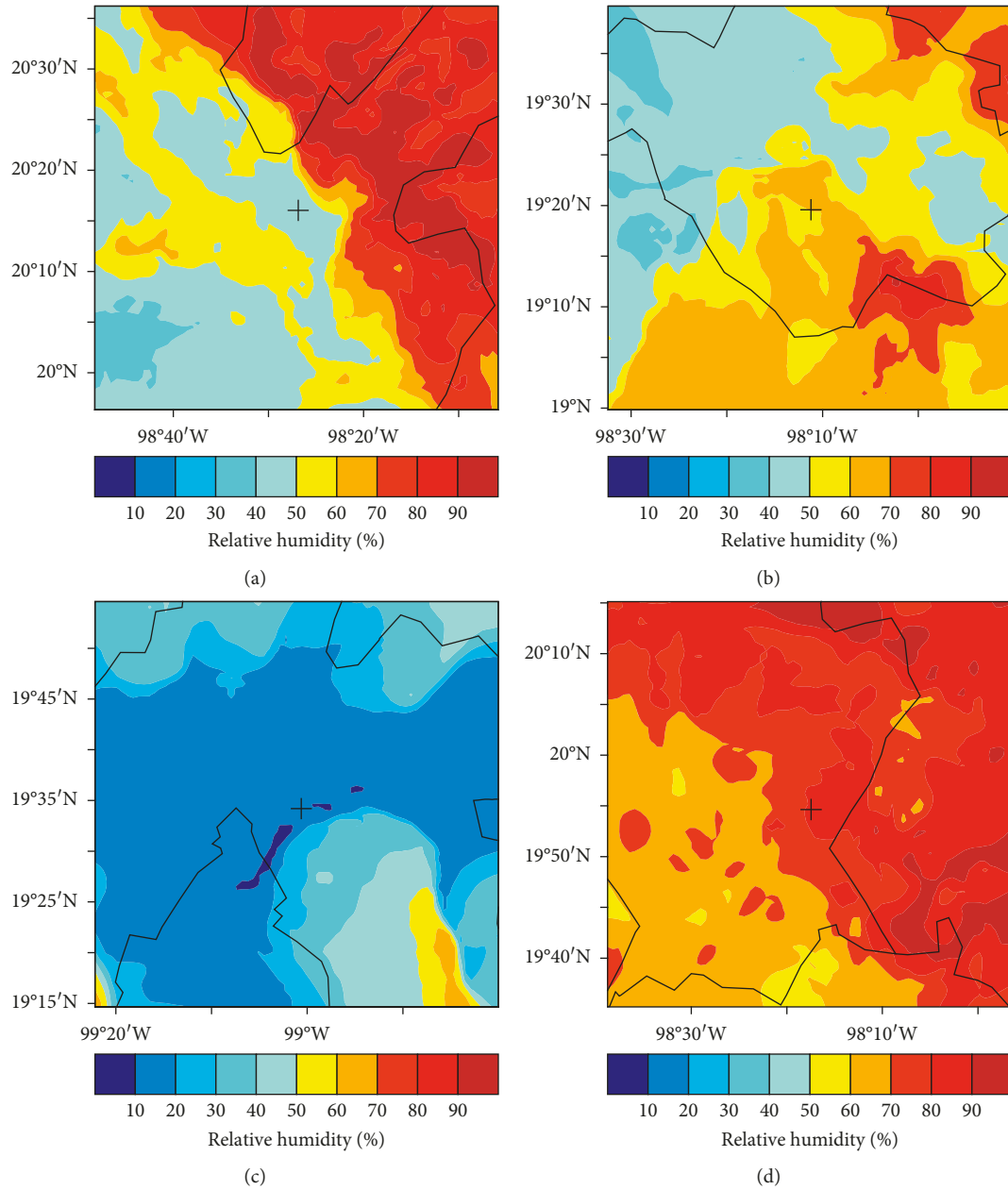
(a)

(b)

(c)

(d)

FIGURE 3: Relative humidity at 2 m calculated for anticyclonic tornadoes (a, b) (I.D. 6 and 9, respectively) and cyclonic tornadoes (c and d) (I.D. 15 and I.D. 20, respectively) (Table 1). The black cross indicates the position of the tornado.

resolutions may not be the most suitable, but the complexity observed in the time series indicates the influence of topography and suggests a similar probability of occurrence of either cyclonic or anticyclonic tornadoes.

The oscillating behaviour of the SRH values of tornadoes in the TMVB can be compared to those calculated for a reference tornado event in Ciudad Acuña, Mexico, on 25 May 2015 (Figure 2). This tornado was generated in a supercell system and occurred in a northern, relatively flat region of Mexico [43]. The difference in the time series generated for this supercell tornado compared to those generated for the tornadoes that formed in the TMVB (1 to 11) is overwhelming. The SRH values for the Ciudad Acuña tornado are always positive, and the curve well behaved.

Atmospheric dynamics in a topographically complex environment include different phenomena such as valley-mountain circulation, convergence and divergence of flows, convection events due to surface heating, forced convection events, pressure gradients associated with mesoscale systems, and cold fronts or tropical waves with high humidity, among others. The interaction of all these factors seems to lead to a disordered pattern of SRH in tornadoes occurring in the TMVB region, as shown in Figure 2. To further verify this finding, the horizontal distribution of SRH was additionally calculated for tornadoes rotating anticyclonically and cyclonically. In Figure 6, SRH integrated between 0 and 1 km for anticyclonic tornadoes in domain D3 is shown. The horizontal
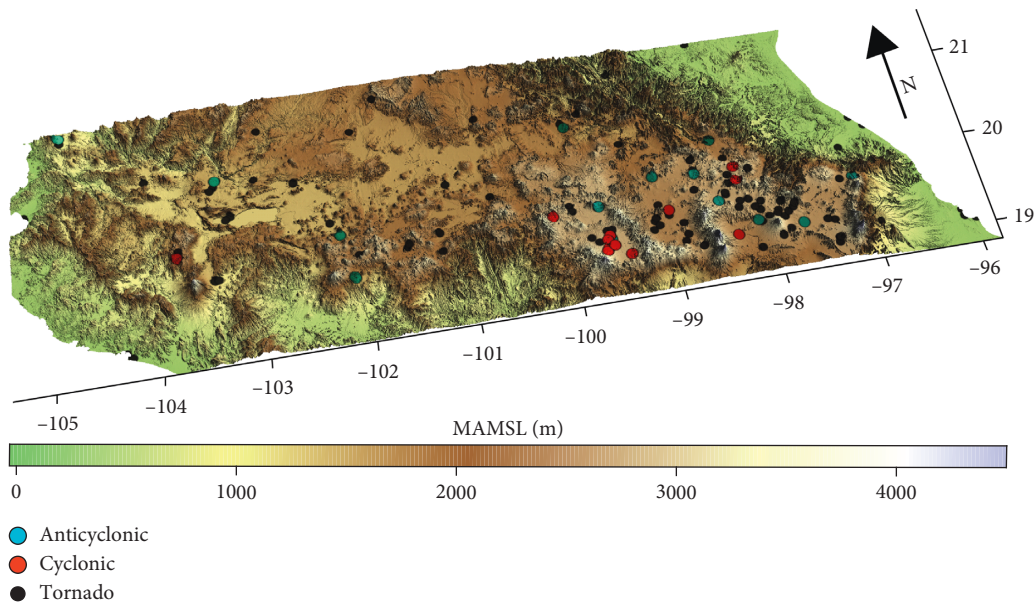
FIGURE 4: Tornado positions in the complex orography of the TMVB. Blue (anticyclonic) and red (cyclonic) points indicate the position of the documented tornadoes where the sense of rotation was determined.
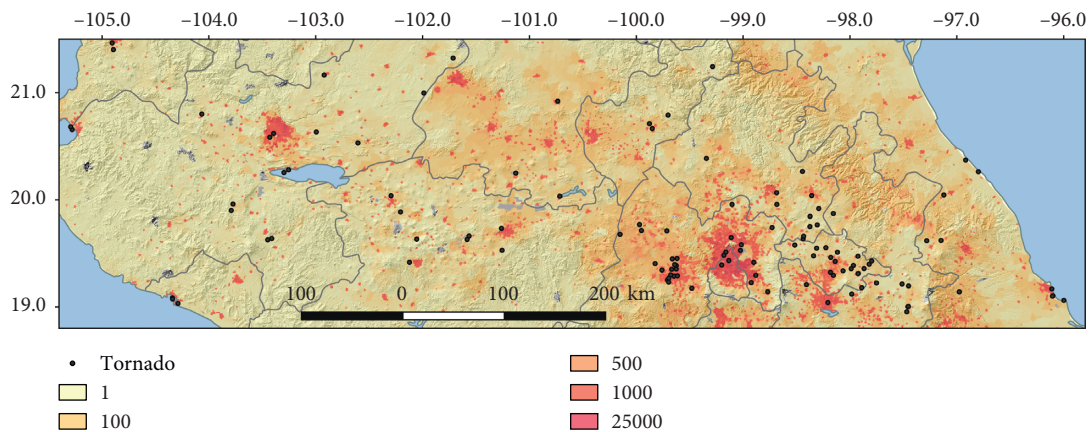

FIGURE 5: Population density (inhabitants per km^2) [39] and position of documented tornadoes.

distribution of SRH values varies widely in terms of positive and negative values. Anticyclonic tornadoes occurred near areas with negative SRH values. However, the SRH values in the vicinity of the four anticyclonic tornadoes vary between -125 and $100 \, \mathrm{m^2 \cdot s^{-2}}$. Notably, the spatial variation in SRH values in the area of tornado occurrence is of the same order as the temporal variation shown in Figure 2. Finally, another interesting finding is the temporal fluctuation in the SRH values of anticyclonic tornadoes, which vary every 30 to 60 minutes (Figure 2).

In addition, the horizontal distribution of SRH values is shown for the cyclonic tornado that developed in Ciudad Acuña (Figure 7(a)) and for three cyclonic tornadoes (Figures 7(b)–7(d)) in the TMVB. The pattern for the first tornado (Figure 7(a)) is completely dominated by a positive SRH system, which is frequent in areas that experience severe supercell storms. This tornado is associated with SRH values mostly oscillating around $350 \, \mathrm{m^2 \cdot s^{-2}}$ over an

extensive area. Some fluctuation is observed, but the area of positive SRH is clearly defined. Also, the SRH pattern of the tornado generated in the supercell (Figure 7(a)) was more ordered than that of tornadoes generated in the complex environment of the TMVB (Figures 7(b)–7(d)). Finally, the SRH values of the tornadoes in the TMVB show greater positive and negative variations in the range of -40 to $140 \, \mathrm{m^2 \cdot s^{-2}}$. The comments and discussion presented above contribute to answering questions about the same probability of rotating clockwise and counterclockwise and why tornadoes rotating in a clockwise direction occur mainly in the TMVB.

6. Conclusions

Tornado phenomena in Mexico exhibit extraordinary characteristics in terms of their sense of rotation, number, and distribution. Moreover, tornadoes in the TMVB region
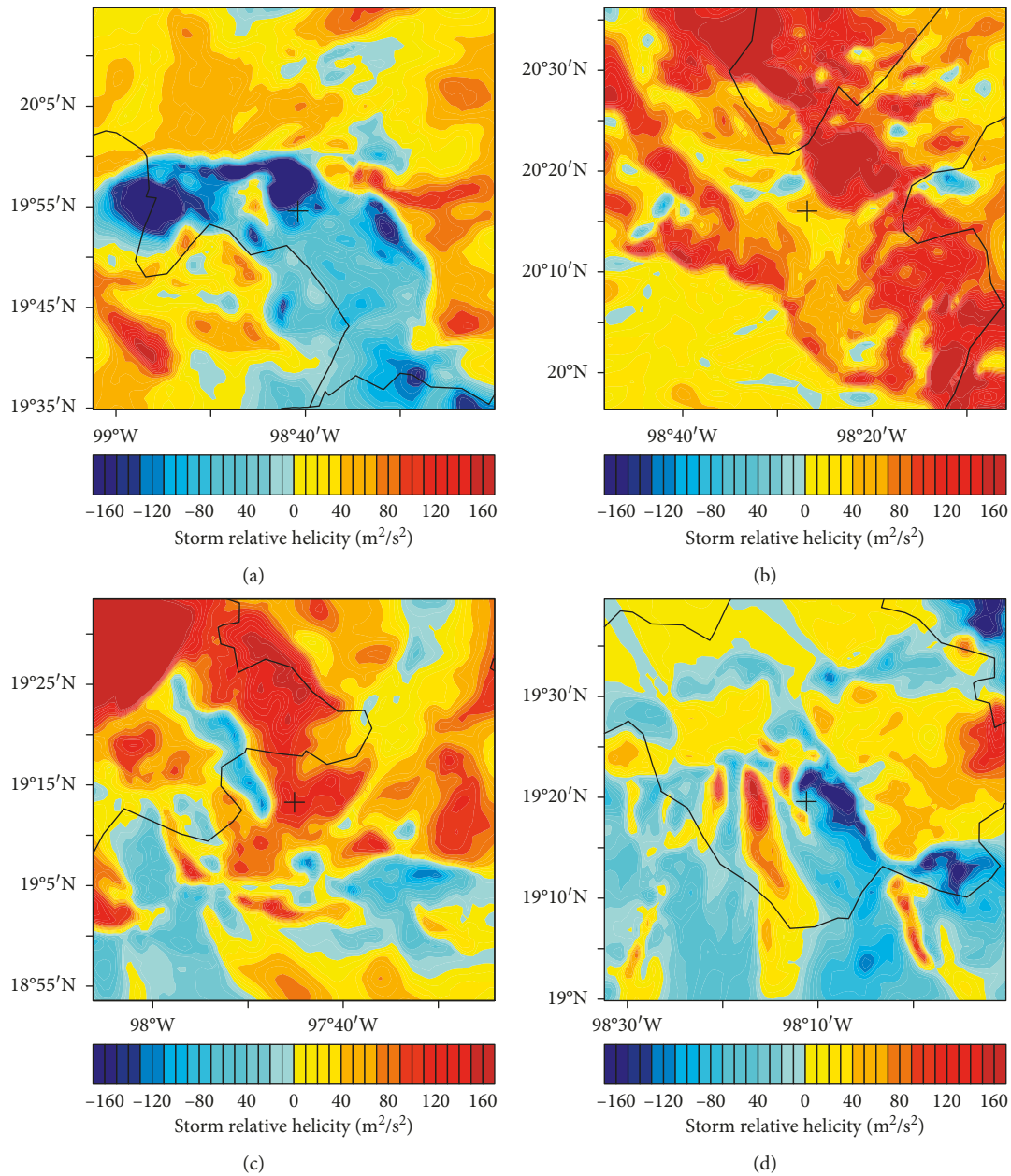
FIGURE 6: Storm relative helicity integrated between 0 and 1 km for anticyclonic tornadoes I.D. 2 (a), I.D. 6 (b), I.D. 7 (c), and I.D. 9 (d) in domain D3 (Table 1 for I.D. numbers). The black crosses indicate the position of the tornadoes.

apparently have a similar probability of cyclonic or anti-cyclonic rotation, suggesting that this behaviour is random and mostly determined by the complex topography, as opposed to dust whirls, for which the random rotation behaviour is mainly determined by turbulent processes. The Coriolis force is about a half than that of the Tornado Alley, and its effect seems to be small. The fact that there is a high percentage of anticyclonic tornadoes confirms that the Coriolis force does not play an important role. This suggests that tornadoes occur in short-lived systems where there is no mesocyclone formation. To explain the observed percentage of 50% of anticyclonic and cyclonic tornadoes, the influence

of the complex orography on the atmospheric circulation in the TMVB prevails. Additionally, a significant number of tornadoes occur in the TMVB region of Mexico, and the number of tornadoes in Mexico is much higher than the one previously thought. Although the statistics presented on tornadoes herein are relatively poor, they are consistent. Our collected data suggest that the number of clockwise-rotating tornadoes may be relatively high in the TMVB. Unfortunately, anticipating where a tornado will hit is one of the most pressing tasks that operative meteorologists and researchers face despite the relative ease of predicting supercell formation [12]. In topographically complex
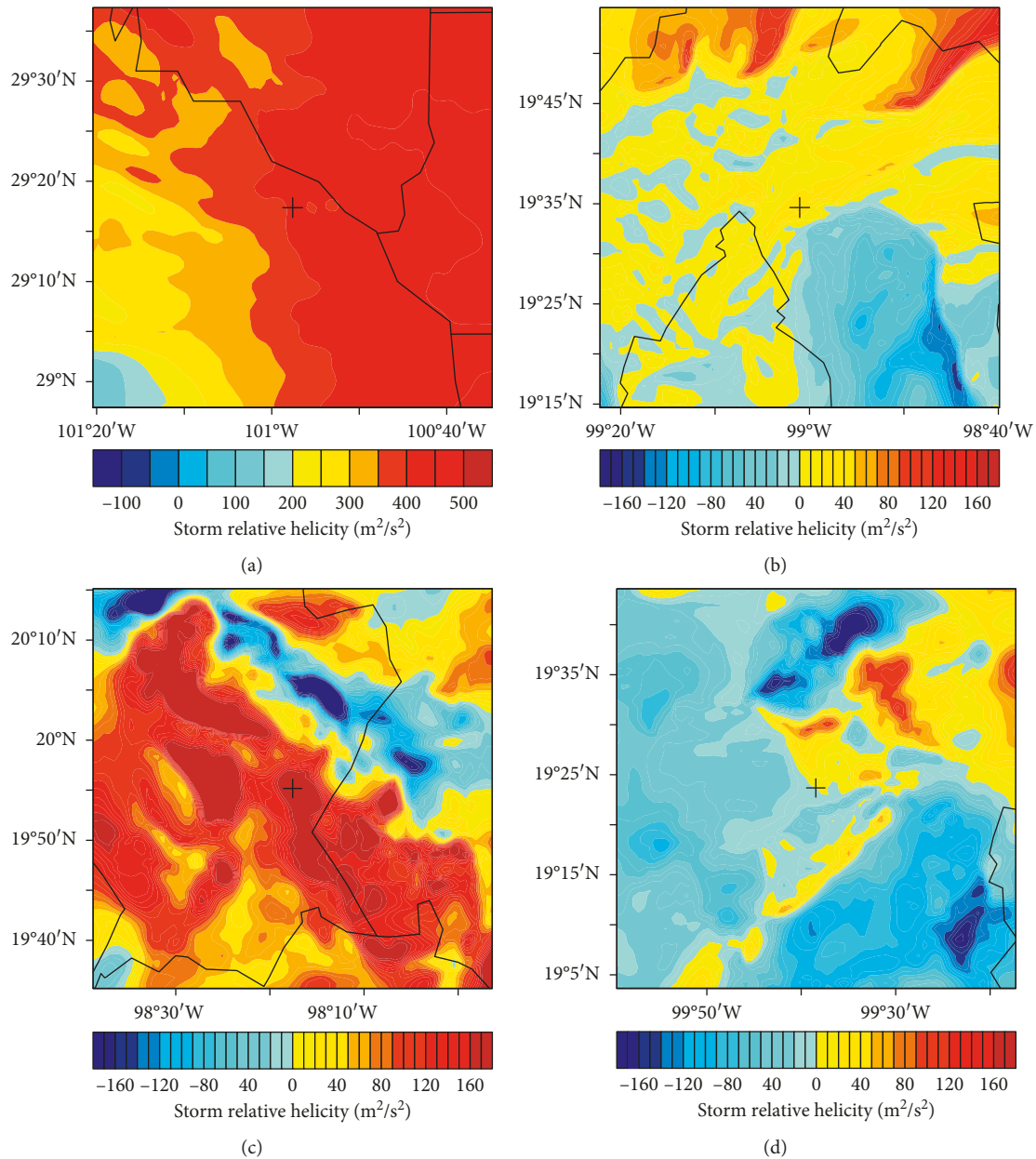
FIGURE 7: Storm relative helicity integrated between 0 and 1 km for cyclonic tornadoes in domain D3. Tornado formed in a supercell system in Ciudad Acuña (a), I.D. 15 (b), I.D. 20 (c), and I.D. 24 (d) (Table 1 for I.D. numbers). The black crosses indicate the position of the tornadoes.

regions, the prediction of where a tornado will hit seems to be an even greater challenge. The main purpose of the VORTEX 2 experiment, funded by the National Science Foundation (NSF) and the National Oceanic Atmospheric Administration (NOAA), is to find answers to how, when, and why tornadoes are formed and to verify the origin of their rotation. Finally, many regions in the world have complex orography, so it would be interesting to explore whether tornadoes in these regions have the same probability of cyclonic or anticyclonic rotation similar to the TMVB. Such studies would also provide further insight into the factors affecting the formation or sense of rotation of tornadoes.

Data Availability

The data used to support the findings of this study are available from the corresponding author upon request.

Conflicts of Interest

The authors declare that there are no conflicts of interest regarding the publication of this paper.

Acknowledgments

We are very grateful for the Mexican individuals who uploaded videos of tornadoes to the Internet, making it possible to formulate several inferences about tornadoes and their sense of rotation in Mexico.

Supplementary Materials

Video links for each tornado case analysed in the TMVB providing rotation evidence are listed in the table (Excel). (*Supplementary Materials*)

References

[1] T. T. Fujita, "Anticyclonic tornadoes," *Weatherwise*, vol. 30, no. 2, pp. 51–64, 1977.

[2] T. S. Glickman and W. Zenk, *Glossary of Meteorology*, American Meteorological Society, Boston, Massachusetts, USA, 2018.

[3] S. C. Bhan, S. Paul, K. Chakravarthy, R. Saxena, K. Ray, and N. K. Gopal, "Climatology of tornadoes over northwest India and Pakistan; and meteorological analysis of recent tornadoes over the region," *Journal of Indian Geophysical Union*, vol. 20, no. 1, pp. 75–88, 2016.

[4] H. E. Brooks, C. A. Doswell III, and M. P. Kay, "Climatological estimates of local daily tornado probability for the United States," *Weather and Forecasting*, vol. 18, no. 4, pp. 626–640, 2003.

[5] P. M. Markowski, E. N. Rasmussen, and J. M. Straka, "The occurrence of tornadoes in supercells interacting with boundaries during VORTEX-95," *Weather and Forecasting*, vol. 13, no. 3, pp. 852–859, 1998.

[6] H. E. Brooks, J. W. Lee, and J. P. Craven, "The spatial distribution of severe thunderstorm and tornado environments from global reanalysis data," *Atmospheric Research*, vol. 67-68, pp. 73–94, 2003.

[7] C. R. Snider, "An anticyclonic tornado," *Monthly Weather Review*, vol. 104, no. 9, pp. 1186-1187, 1976.

[8] J. P. Monteverdi, W. Blier, G. Stumpf, W. Pi, and K. Anderson, "First WSR-88D Documentation of an anticyclonic supercell with anticyclonic tornadoes: the sunnyvale-Los Altos, California, tornadoes of 4 may 1998," *Monthly Weather Review*, vol. 129, no. 11, pp. 2805–2814, 2001.

[9] M. J. Bunkers and J. W. Stoppkotte, "Documentation of a rare tornadic left-moving supercell," *E-Journal of Severe Storms Meteorology*, vol. 2, no. 2, 2007.

[10] C. A. Doswell and D. W. Burgess, "Tornadoes and tornadic storms: a review of conceptual models," in *The Tornado: Its Structure, Dynamics, Prediction, and Hazards*, C. Church, D. Burgess, C. Doswell, and R. Davies-Jones, Eds., pp. 161–172, American Geophysical Union, Washington, DC, USA, 1993.

[11] R. Davies-Jones, R. J. Trapp, and H. B. Bluestein, "Tornadoes and tornadic storms," in *Severe Convective Storms*, C. A. Doswell, Ed., pp. 167–221, American Meteorological Society, Boston, MA, USA, 2001.

[12] P. Markowski, "Tornadoes and tomadogenesis," in *Atmospheric Convection Research and Operational Forecasting Aspects*, Springer, Berlin, Germany, 2007.

[13] H. B. Bluestein, *Severe Convective Storms and Tornadoes: Observations and Dynamics*, Springer, Berlin, Germany, 2013.

[14] National Centers for Environmental Information, *U.S. Tornado Climatology*, 2017, https://www.ncdc.noaa.gov/climate-information/extreme-events/us-tornado-climatology.

[15] S. M. Verbout, H. E. Brooks, L. M. Leslie, and D. M. Schultz, "Evolution of the US tornado database: 1954-2003," *Weather and Forecasting*, vol. 21, no. 1, pp. 86–93, 2006.

[16] D. Etkin, S. E. Brun, A. Shabbar, and P. Joe, "Tornado climatology of Canada revisited: tornado activity during different phases of ENSO," *International Journal of Climatology*, vol. 21, no. 8, pp. 915–938, 2001.

[17] A. J. Litta, U. C. Mohanty, and S. C. Bhan, "Numerical simulation of a tornado over Ludhiana (India) using WRF-NMM model," *Meteorological Applications*, vol. 17, no. 1, pp. 64–75, 2010.

[18] P. T. Nastos and J. T. Matsangouras, "Tornado activity in Greece within the 20th century," *Advances in Geosciences*, vol. 26, pp. 49–51, 2010.

[19] Y. Yao, X. Yu, Y. Zhang et al., "Climate analysis of tornadoes in China," *Journal of Meteorological Research*, vol. 29, no. 3, pp. 359–369, 2015.

[20] M. Gayà, "Tornadoes and severe storms in Spain," *Atmospheric Research*, vol. 100, no. 4, pp. 334–343, 2011.

[21] M. A. Silva Dias, "An increase in the number of tornado reports in Brazil," *Weather, Climate, and Society*, vol. 3, no. 3, pp. 209–217, 2011.

[22] E. de Coning and B. F. Adam, "The tornadic thunderstorm events during the 1998–1999 South African summer," *Water*, vol. 26, no. 3, pp. 361–376, 2000.

[23] L. Ferrari, M. López-Martínez, G. Aguirre-Díaz, and G. Carrasco-Núñez, "Space-time patterns of Cenozoic arc volcanism in central Mexico: from the Sierra Madre Occidental to the Mexican Volcanic Belt," *Geology*, vol. 27, no. 4, pp. 303–306, 1999.

[24] J. J. Morrone, T. Escalante, and G. Rodríguez-tapia, "Mexican biogeographic provinces: map and shapefiles," *Zootaxa*, vol. 4277, no. 2, pp. 277–279, 2017.

[25] J. M. Medrano and A. A. García, "Climatología de tornados en México," *Investigaciones Geográficas, Boletín del Instituto de Geografía*, vol. 83, pp. 74–87, 2014.

[26] W. C. Skamarock, J. B. Klemp, J. Dudhia et al., "A description of the advanced research WRF version 3," NCAR Tech Notes-475 +STR, 2008.

[27] C. M. Shafer, A. E. Mercer, C. A. Doswell III, M. B. Richman, and L. M. Leslie, "Evaluation of WRF forecasts of tornadic and nontornadic outbreaks when initialized with synoptic-scale input," *Monthly Weather Review*, vol. 137, no. 4, pp. 1250–1271, 2009.

[28] J. Mercader, B. Codina, A. Sairouni, and J. Cunillera, "Results of the meteorological model WRF-ARW over Catalonia, using different parameterizations of convection and cloud microphysics," *Journal of Weather and Climate of the Western Mediterranean*, vol. 7, pp. 75–86, 2010.

[29] I. T. Matsangouras, P. T. Nastos, and I. Pytharoulis, "Synoptic-mesoscale analysis and numerical modeling of a tornado event on 12 February 2010 in northern Greece," *Advances in Science and Research*, vol. 6, no. 1, pp. 187–194, 2011.

[30] J. S. Kain, S. J. Weiss, J. J. Levit, M. E. Baldwin, and D. R. Bright, "Examination of convection-allowing configurations of the WRF model for the prediction of severe convective weather: the SPC/NSSL Spring Program 2004," *Weather and Forecasting*, vol. 21, no. 2, pp. 167–181, 2006.

[31] National Centers for Environmental Prediction, National Weather Service, National Oceanic and Atmospheric Administration, and US Department of Commerce, *NCEP FNL Operational Model Global Tropospheric Analyses, Continuing From July 1999*, Research Data Archive at the National Center

for Atmospheric Research, Computational and Information Systems Laboratory, 2000.

[32] S. Y. Hong, J. Dudhia, and S. H. Chen, "A revised approach to ice microphysical processes for the bulk parameterization of clouds and precipitation," *Monthly Weather Review*, vol. 132, no. 1, pp. 103–120, 2004.

[33] J. Dudhia, "Numerical study of convection observed during the winter monsoon experiment using a mesoscale two-dimensional model," *Journal of the Atmospheric Sciences*, vol. 46, no. 20, pp. 3077–3107, 1989.

[34] E. J. Mlawer, S. J. Taubman, P. D. Brown, M. J. Iacono, and S. A. Clough, "Radiative transfer for inhomogeneous atmospheres: RRTM, a validated correlated-k model for the longwave," *Journal of Geophysical Research: Atmospheres*, vol. 102, no. D14, pp. 16663–16682, 1997.

[35] C. A. Paulson, "The mathematical representation of wind speed and temperature profiles in the unstable atmospheric surface layer," *Journal of Applied Meteorology*, vol. 9, no. 6, pp. 857–861, 1970.

[36] M. Tewari, F. Chen, W. Wang et al., "Implementation and verification of the unified NOAH land surface model in the WRF model," in *Proceedings of 20th Conference on Weather Analysis and Forecasting and the 16th Conference on Numerical Weather Prediction*, vol. 1115, Phoenix, AZ, USA, January 2004.

[37] S. Y. Hong, Y. Noh, and J. Dudhia, "A new vertical diffusion package with an explicit treatment of entrainment processes," *Monthly Weather Review*, vol. 134, no. 9, pp. 2318–2341, 2006.

[38] J. S. Kain, "The Kain–Fritsch convective parameterization: an update," *Journal of Applied Meteorology*, vol. 43, no. 1, pp. 170–181, 2004.

[39] Center for International Earth Science Information Network (CIESIN) of Columbia University, *Gridded Population of the World, Version 4 (GPWv4): Population Density, Revision 10*, NASA Socioeconomic Data and Applications Center (SEDAC), Palisades, NY, USA, 2017.

[40] W. S. Wu, D. K. Lilly, and R. M. Kerr, "Helicity and thermal convection with shear," *Journal of the Atmospheric Sciences*, vol. 49, no. 19, pp. 1800–1809, 1992.

[41] E. Agee and E. Jones, "Proposed conceptual taxonomy for proper identification and classification of tornado events," *Weather and Forecasting*, vol. 24, no. 2, pp. 609–617, 2009.

[42] E. N. Rasmussen, "Refined supercell and tornado forecast parameters," *Weather and Forecasting*, vol. 18, no. 3, pp. 530–535, 2003.

[43] J. F. León-Cruz, N. Carbajal, and L. F. Pineda-Martínez, "Meteorological analysis of the tornado in Ciudad Acuña, Coahuila State, Mexico, on May 25, 2015," *Natural Hazards*, vol. 89, no. 1, pp. 423–439, 2017.
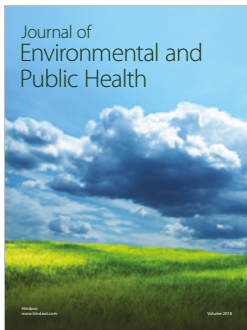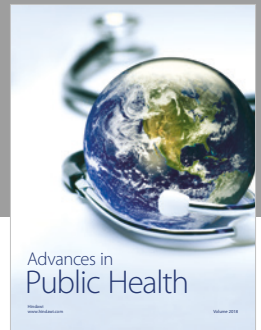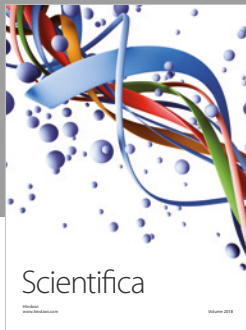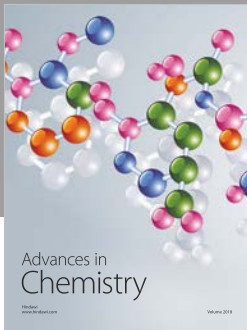
Submit your manuscripts at
www.hindawi.com